Appl. Math. and Comp. Sci., 1992, vol.2, No.1, 87–118

FAULT DETECTION IN COAL FIRED POWER PLANTS USING NONLINEAR FILTERING

ZOHREH FATHI*, JÓZEF KORBICZ**, W. FRED RAMIREZ*

On the contrary to many recent attempts using knowledge–based system techniques where diagnostic analysis is based solely on measurable and observable data, in this work we propose to investigate the adaptive inclusion of a state and/or parameter estimation module in the diagnostic reasoning loop, in addition to employing information based on measurable data. The design methodology is a new layered knowledge base that houses heuristics knowledge in the high–levels and the process–general estimation knowledge in the low–levels. The purpose of this paper is to present the failure detection issues of the deaerator control subsystem for the coal fired power plant. The main emphasis is placed upon the model–based redundancy methods which create the low–levels of the knowledge base. Due to the highly nonlinear nature of the power plant dynamic, the modified extended Kalman filters are designed for use as detection filters. The developed approach is shown to be effective in detecting and isolating failures of a subsystem of a power plant with an appropriate degree of complexity.

Introduction

Process fault detection and diagnosis is important from both a theoretical and practical viewpoint. The increasing complexity of process plants such as the nuclear power plants or aerospace vehicles systems, and a growing demand for fault–tolerance encourage industry to look for new methods and techniques for detecting and diagnosing process abnormalities. To date many fault detection and diagnosis methods have been proposed for dynamical systems. Several surveys of these approaches exist (Willsky, 1976; Isermann, 1984; Frank, 1990; Korbicz *et al.*, 1991). More comprehensive sources are the excellent book edited by Patton *et al.*, (1989) and the preprints of the IFAC/IMACS symposium SAFEPROCESS'91 (Germany, 1991) for the fault detection and isolation techniques mainly based on the use of mathematical models of process systems.

In general, various known approaches to the fault detection and isolation (FDI) problems using analytical redundancy can be traced back to a few basic concepts.

* Department of Chemical Engineering, University of Colorado, Boulder, Colorado, U.S.A.
** Department of Computer Science, Higher College of Engineering, Zielona Góra, Poland

Among these are: the detection filter (Jones, 1973), the innovation test using Kalman filters or Luenberger observers (Yoshimura *et al.*, 1979; Watanabe and Himmelblau, 1982), the generalised parity space approach (Gertler and Singer, 1990; Luck and Ray, 1991; Patton and Chen, 1991), the parameter estimation technique (Isermann, 1984), signal processing (Yung and Clarke, 1989), statistical tests (Chien and Adams, 1976; Kerr, 1982), Petri nets approach (Prock, 1991), the expert system applications (Tzafestas, 1989; Neumann, 1990), and the neural networks applications (Naidu *et al.*, 1990; Yao and Zafiriou, 1990; Sorsa and Koivo, 1991).

Among the above mentioned methods and techniques are the expert system and neural network approaches, which are especially interesting and important from a practical point of view. They can complement the existing analytical and algorithmic methods of fault detection by application of artificial intelligence (Miller *et al.*, 1990; Kramer and Leonard, 1990; Johannsen and Alty, 1991). The main advantage of expert system approach lies in fact that it makes use of qualitative models, based on the available knowledge of the system. The combination of both strategies allows the use of all available information given by numeric and symbolic models for performing the fault detection and diagnosis task.

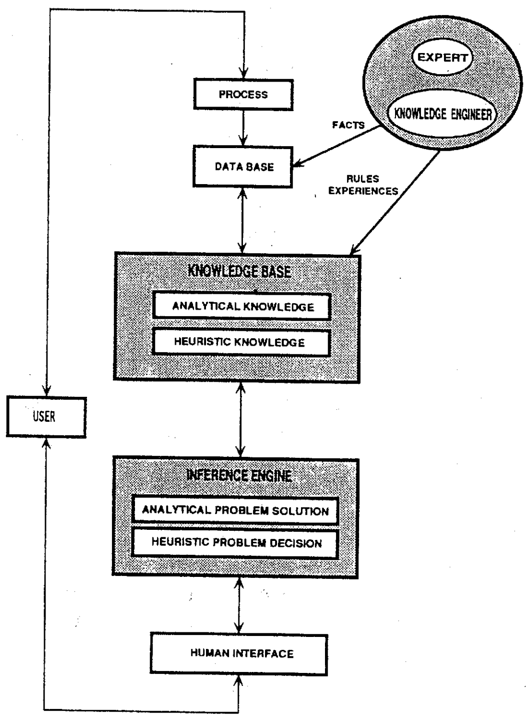

Fig. 1. Framework of the knowlege base.

This work considers an integrated approach based on combining the analytically–redundant FDI schemes and the knowledge–based techniques. The overall structure of our diagnostic methodology of embedding estimation based techniques within the framework of a knowledge base is represented in Figure 1. The raw data are fed to a fault detector (a preprocessor) which performs statistical tests to identify the process condition (normal or abnormal). The preprocessor is basically an alarm system that is used to trigger the initiation of the knowledge–based system. The task of the knowledge base is to determine the source and extent of the true fault. Both a state/parameter estimator and a statistical analyzer are included in the loop of diagnostic reasoning. The design methodology is a hierarchical knowledge structure with compiled knowledge at higher levels of abstraction and analytical redundancy at lower levels of abstraction. This integrated approach reduces the computational complexity associated with functionally–redundant schemes and increases the effectiveness of the knowledge–based approach.

It is beyond the scope of this paper to discuss the knowledge–based redundancy problems in detail. The main emphasis is placed upon the model–based redundancy problems. First, a brief description of the deaerator control subsystem of a coal–fired power plant and its mathematical model are given. Then, the estimation–based approach to FDI is presented. Due to the highly nonlinear nature of the power plant dynamics, the modified extended Kalman filters are designed for use as detection filters. These analytical algorithms create the low–levels of the knowledge base. The design of local filters and simulation results for the power plant subsystem illustrating the validity of the implemented filters are shown in the last section.

1. Process Description and Model Formulation

The process schematic shown in Figure 2 represents the plant components and flow paths selected for prototype diagnostic system development. This diagram shows the condensate pump, the control valve, the deaerator level controller, the extraction steam pipe, and the deaerator and its storage tank. It does not include the low–pressure feedwater heaters; they are represented only as a flow resistance between the control valve and the deaerator. The objective is the analysis of problems associated with the transportation lines, the deaerator, and its control system.

The mathematical model for each component consists of conservation of mass, conservation of energy, fluid mechanics, and fluid properties. In the following, each component is briefly described and only the more representative equations are presented.

1.1. Valve

The valve is primarily used for modulating to control the flow rate through the valve for maintaining the liquid level in the deaerator storage tank. The basic

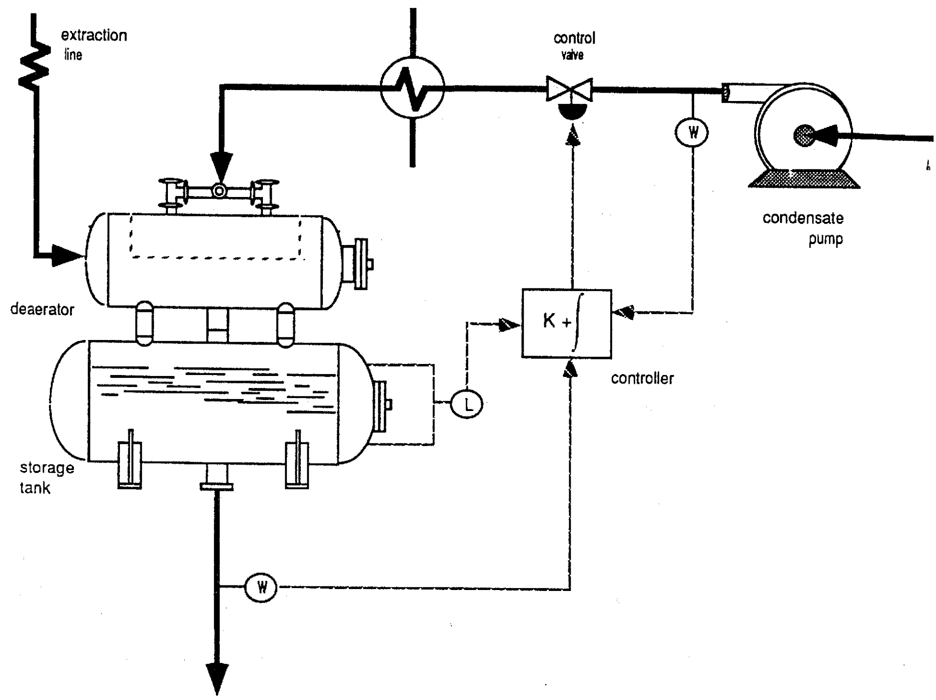

Fig. 2. Process schematic.

assumptions used in modeling the valve are quasi-steady state, adiabatic, no seal leakage, and no reverse flow.

On writing a steady-state mechanical energy balance for the valve with a constant density fluid and solving for the mass flow rate, we have

$$w_p = C_v \left[\rho_{pv}\left(P_p - P_v\right) + \rho_{pv}^2 \Delta H_v / 144\right]^{1/2} \tag{1}$$

where C_v is valve conductance, P_p is pressure of water leaving pump and entering valve ($psia$), P_v is pressure of water leaving valve ($psia$), w_p is mass flow rate of water leaving pump and entering valve (lb_m/hr), ΔH_v is difference in elevation between inlet and outlet (ft), and ρ_{pv} is average of upstream and downstream fluid densities (lb_m/ft^3).

Since the low-pressure heaters are only modeled as a flow resistance, the valve conductance can be combined with the flow conductance of the pipe associated with the heaters. Upon combining the valve conductance, C_v, and the pipe conductance, C_p, in series, the equivalent conductance is

$$C_{eq} = 1/\sqrt{(1/C_v)^2 + (1/C_p)^2} \tag{2}$$

The valve conductance, C_v, varies with valve stroke according to its inherent valve characteristics (equal percentage, linear, or quick opening).

1.2. Extraction Pipe

This pipe is the interconnecting component between the turbine and the deareator. The extraction steam flows through this pipe before entering the deaerator. The primary phenomenon to be modeled is pressure losses due to friction and elevation. The friction factor is a function of Reynold's number and pipe roughness. However, for a given pipe roughness and turbulent flow, the friction factor can be assumed constant. The basic assumptions used in developing the model are: quasi-steady state, single-phase flow, fully-developed turbulent flow, and no reverse flow.

Using the quasi-steady state assumption and replacing the fluid density by the average of the upstream and downstream values, the mechanical energy balance for the extraction pipe can be solved for the mass flow rate as

$$w_e = C_f \left[\rho_{se} \ (P_s - P_e) + \rho_{se}^2 \Delta H_{se}/144\right]^{1/2} \tag{3}$$

where C_f is flow conductance, P_s is pressure of steam entering pipe ($psia$), P_e is pressure of steam leaving pipe ($psia$), w_e is mass flow rate of steam leaving pipe (lb_m/hr), ΔH_{se} is elevation difference between upstream and downstream segments (ft), and ρ_{se} is average of downstream and upstream fluid densities (lb_m/ft^3).

1.3. Deaerator

The deaerator subsystem is composed of a deaerator (an open feedwater heater) and its storage tank. Deaerators serve four major tasks: i) removal of noncondensable gases to prevent corrosion and scaling of boiler surfaces due to gases dissolved in the feedwater, ii) heating of feedwater, iii) provide feedwater storage, and iv) are located to provide a substantial net positive suction head on the boiler feed pumps, preventing pump cavitation.

The feedwater is heated by spraying into a steam space. Most of the gases are relased at this point due to the higher solubility of gases in steam than in water. The remaining deaeration takes place in the stack of trays or baffles. Steam with a high concentraction of dissolved gases is vented into the atmosphere (since the amount of vented steam is small, this effect is neglected). The heated and deaerated feedwater is then collected in storage tank below the deaerating section. The storage tank generally maintains sufficient storage to allow the plant to withstand an interruption of the condensate. It also serves to provide surge protection for the boiler feed pumps. The water level in the storage tank is maintained at a desired set point through a control valve placed on the condensate flow section upstream from the deaerator.

The major phenomena simulated are: phase equilibrium, feedwater heating and deaeration, and elevation head. The mathematical model consists of conservation of mass, conservation of thermal energy, mechanical energy balance, fluid properties (steam table), and geometrical relations. The basic assumptions in model development are: phase equilibrium between liquid and vapor phases, equal pressure in the deaerating section and the storage tank, and negligible non–condensable gas effects.

For a fixed control volume, the mass conservation relation can be written as

$$\frac{d\rho_d}{dt} = (\omega_{d_{in}} - \omega_{d_{out}})/V_{tm} \tag{4}$$

where ρ_d is the bulk density over entire vessel (lb_m/ft^3), $\omega_{d_{in}}$ is the mass flow rate of feedwater and steam entering deaerator (lb_m/hr), $\omega_{d_{out}}$ is the mass flow rate of fluid leaving deaerator (lb_m/hr), $V_{tm} = 3600V_t$, and V_t is the total volume of deaerating and storage tanks (ft^3).

For no heat transfer and negligible kinetic energy effects, the energy balance gives

$$\frac{du_d}{dt} = \left(\omega_{d_{in}} h_{d_{in}} - \omega_{d_{out}} h_{d_{out}} - V_{tm} u_d \frac{d\rho_d}{dt}\right) / (\rho_d V_{tm}) \tag{5}$$

where u_d is the bulk specific internal energy (Btu_m/lb_m), $h_{d_{in}}$ is the enthalpy of feedwater and steam entering deaerator (Btu_m/lb_m), and $h_{d_{out}}$ is the enthalpy of fluid leaving deaerator (Btu_m/lb_m).

Through the use of $h_d = u_d + \gamma\rho_d^{-1} P_d$, equations (4) and (5) are transformed to the following form for the bulk specific enthalpy, h_d, and the deaerator pressure, P_d,

$$\begin{aligned}\frac{dh_d}{dt} &= [(-h_d + \gamma\alpha_p^{-1})(\omega_{d_{in}} - \omega_{d_{out}}) + \omega_{d_{in}} h_{d_{in}} - \omega_{d_{out}} h_{d_{out}}]/ \\ &\quad [V_{tm}(\rho_d + \gamma\alpha_{hp})]\end{aligned} \tag{6}$$

$$\frac{dP_d}{dt} = -\alpha_{hp}\frac{dh_d}{dt} + (\omega_{d_{in}} - \omega_{d_{out}})/(V_{tm}\alpha_p) \tag{7}$$

where $\alpha_{hp} = \alpha_h/\alpha_p$, $\alpha_h = \left.\frac{\partial\rho_d}{\partial h_d}\right|_{P_d=\text{const}}$, $\alpha_p = \left.\frac{\partial\rho_d}{\partial P_d}\right|_{h_d=\text{const}}$, and γ is the conversion factor equivalent to 0.1851 $(Btu \cdot in^3)/(lb_f \cdot ft^3)$.

The water level in the deaerator is determined by a mass accounting in the deaerating and the storage sections,

$$L = D\,\frac{(\rho_d - \rho_g)}{(\rho_f - \rho_g)}\,(V_t/V_s) \tag{8}$$

where L is liquid level (*inches*), D is diameter of storage tank (*inches*), V_s is volume of storage tank (ft^3), ρ_f is density of saturated liquid (lb_m/ft^3), and ρ_g is density of saturated vapor (lb_m/ft^3).

1.4. Controller

The deaerator level controller is a three–mode proportional–integral controller with anti–reset windup. A limit to the integral demand is provided to prevent the integral action from continuing to intergrate past a certain point so that the integral action is active as soon as the control error reverses.

The error signal for the three–mode deaerator level controller that is direct acting (the output increases with an increase in setpoint) is defined as

$$\varepsilon = \underbrace{k_1(L_s - L_m) + k_2\omega_{d_{out}}}_{\longleftarrow\ demand\ \longrightarrow} \quad \underbrace{-\ k_3\omega_c}_{\leftarrow\ supply\ \rightarrow} \tag{9}$$

where ε is the control error signal, L_s is the deaerator level setpoint (*inches*), L_m is the deaerator level measured (*inches*), ω_c is the mass flow rate of condensate water (lb_m/hr), $\omega_{d_{out}}$ is the mass flow rate of water leaving deaerator (lb_m/hr), and k_1, k_2, and k_3 are constant parameters.

The proportional and integral actions on the error signal are expressed as

$$O_P = k_p\varepsilon \tag{10}$$

$$\frac{dO_I}{dt} = k_I \left\{\varepsilon + k_a[\min(O_h–O_T,\ 0) + \max(O_\ell–O_T,\ 0\right\} \tag{11}$$

where O_P is proportional output (fraction), k_p is proportional gain, O_I is integrator output (fraction), k_I is integrator gain ($seconds^{-1}$), k_a is gain on anti–reset windup, O_T is unbounded controller output, O_h is higher limit on controller output, and O_ℓ is lower limit on controller output. The unbounded controller output is the sum of the proportional and integral actions (the actual output is the bounded O_T).

$$O_T = O_P + O_I \tag{12}$$

2. State and/or Parameter Estimators Design

Most of the work considering the problem of FDI from the point of analytical redundancy propose to use the Kalman filter in the stochastic case, and the Luenberger observer in the deterministic case (Willsky *et al.*, 1974; Wilsky and Jones, 1976; Kerr, 1982; Yoshimura *et al.*, 1979; Tylee, 1982; Watanabe and Himmelblau, 1983; Laparo *et al.*, 1991). Here, we base the design of our detectors on two concepts:

structural decomposition and adaptive Kalman filtering. That is, the plant structure is decomposed into units for which individual filters are designed. In general, the design of local filters can range from one incorporating most likely fault modes to one incorporating all possible ones.

Due to mixed dynamic modes (slow and fast) common in most applications, the modified extended Kalman filter (Fathi *et al.*, 1991) is used for designing the detection filters. These analytical algorithms are housed at the low levels of abstraction of a hierarchical knowledge structure. In the following, first the modified extended Kalman filter algorithm and then a statistical test for checking the filter behavior are presented.

2.1. Nonlinear Filtering for Systems With Coupled Static and Dynamic Models

In the following, the Kalman filter approach will be presented with a brief description on its use for fault detection problems. No attempt is made to derive the Kalman filter equations. Several excellent texts (Anderson and Moore, 1979; Sorenson, 1985) provide such derivations. Some special problems of the Kalman filter applications have been treated by Fathi *et al.*, (1991), and Korbicz and Zgurovsky (1991).

Different nonlinear techniques for solving the problem of state estimation are available (Anderson and Moore, 1979; Sorenson, 1985) and a short survey of the recursive state estimation techniques is given by Misawa and Hendrick (1988). Among these techniques, the Extended Kalman Filter (EKF) method is widely used by most investigators to solve practical problems (Sorenson, 1985; Loparo *et al.*, 1986; Tsuge *et al.*, 1991). Therefore this suboptimal filter is used in the design of state and parameter estimators.

From the process model presented in the previous section, it is clear that the model equations are nonlinear and consist of both static and dynamic equations. Thus, it is important to consider the application of the EKF algorithm to the joint parameter and state estimation for systems with coupled static and dynamic models.

Let the model of a general stochastic system with unknown parameter vector $\boldsymbol{\theta}$ be described mathematically by the following equations (Fathi *et al.*, 1991)

$$\boldsymbol{x}_d(k+1) = \boldsymbol{f}_d(k, \boldsymbol{x}_d(k), x_s(k), \boldsymbol{\theta}(k), \boldsymbol{u}(k)) + \boldsymbol{w}_d(k) \tag{13}$$

$$0 = \boldsymbol{f}_s(k+1, \boldsymbol{x}_d(k+1), \boldsymbol{x}_s(k+1), \boldsymbol{\theta}(k+1), \boldsymbol{u}(k+1)) + \boldsymbol{w}_s(k+1) \tag{14}$$

$$\boldsymbol{y}(k+1) = \boldsymbol{h}(k+1, \boldsymbol{x}_d(k+1), \boldsymbol{x}_s(k+1), \boldsymbol{\theta}(k+1), \boldsymbol{u}(k+1)) + \boldsymbol{v}(k+1) \tag{15}$$

where equations (13) and (14) describe the dynamic and static models, respectively, and equation (15) is the measurement model, $\boldsymbol{u}(k)$ is known input, $\boldsymbol{v}(k)$ is additive measurement noise, $\boldsymbol{w}(k)$ is additive process noise, $\boldsymbol{x}_d(k)$ is system state with slow dynamics, $\boldsymbol{x}_s(k)$ is system state with fast dynamics, $\boldsymbol{y}(k)$ is output vector (observable signals), and $\boldsymbol{\theta}(k) = [\ \boldsymbol{c}^T(k)\ \ \boldsymbol{d}_u^T(k)\ ]$; $\boldsymbol{c}$ and $\boldsymbol{d_u}$ are physical coefficients and unmeasured disturbances, respectively. Sub–indices d and s denote variables and parameters associated with slow and fast dynamics, respectively.

Furthermore, it is assumed that the system noises $\boldsymbol{w}_d(k)$ and $\boldsymbol{w}_s(k+1)$, the measurement noise $\boldsymbol{v}(k)$, and the initial conditions $\boldsymbol{x}_d^0$ and $\boldsymbol{x}_s^0$ are random variables with known statistics

$$\begin{aligned}
&E[\boldsymbol{w}_i(k)] = 0 \qquad E[\boldsymbol{v}(k)] = 0 \qquad E[\boldsymbol{x}_i^0] = \hat{\boldsymbol{x}}_i^0 \\
&E[\boldsymbol{w}_i(k)\boldsymbol{w}_i^T(l)] = \boldsymbol{Q}_i(k)\delta_{kl}, \quad E[\boldsymbol{v}(k)\boldsymbol{v}^T(l)] = \boldsymbol{R}(k)\delta_{kl}, \\
&E[\delta\boldsymbol{x}_i^0(\delta\boldsymbol{x}_i^0)^T] = \boldsymbol{P}_i(0|0)
\end{aligned} \tag{16}$$

where ^{T} denotes the transpose operator, δ_{kl} is the Kronecker delta function, $\delta\boldsymbol{x}_i^0 = \boldsymbol{x}_i^0 - \widehat{\boldsymbol{x}}_i^0$, $\boldsymbol{P}(0|0)$ and $\boldsymbol{Q}(k)$ are symmetric non–negative definite matrices, $\boldsymbol{R}(k)$ is a symmetric positive definite matrix, and $i = d, s$. In addition, it is assumed that $\boldsymbol{w}_i(k)$, $\boldsymbol{v}(k)$, and $\boldsymbol{x}_i^0$ are uncorrelated.

To cope with time–varying parameters, we postulate that the true parameter vector $\boldsymbol{\theta}$ varies according to

$$\boldsymbol{\theta}(k+1) = \boldsymbol{\theta}(k) + \boldsymbol{\omega}_\theta(k) \tag{17}$$

where $\boldsymbol{\omega}_\theta(k)$ is the parameter noise with zero mean and $\boldsymbol{Q}_\theta$ covariance matrix.

To tackle the joint state and parameter estimation problem, the augmented state vector $\boldsymbol{z}$, is defined as

$$\boldsymbol{z}^T(k) \stackrel{\Delta}{=} \left[\boldsymbol{x}_d^T(k)\ \ \boldsymbol{x}_s^T(k)\ \ \boldsymbol{\theta}^T(k)\right] \tag{18}$$

To solve the joint state and parameter estimation problem for the augmented system described by equations (13)–(15) and (17), the nonlinear Kalman filter approach (Bryson and Ho, 1975; Anderson and Moore, 1979) can be applied. Based on the measurement sequence $\boldsymbol{Y}(k) = \{\boldsymbol{y}(0), \boldsymbol{y}(1), ..., \boldsymbol{y}(k)\}$, the modified EKF algorithm is given by the sequential use of the following recursive algorithm (Fathi *et al.*, 1991)

$$\widehat{\boldsymbol{x}}_d(k+1|k) = \boldsymbol{f}_d(k, \widehat{\boldsymbol{x}}_d(k|k), \widehat{\boldsymbol{x}}_s(k|k), \widehat{\boldsymbol{\theta}}(k|k), \boldsymbol{u}(k)) \tag{19}$$

$$\begin{aligned}
\widehat{\boldsymbol{x}}_s(k+1|k) = \mathrm{Sol}_{\widehat{\boldsymbol{x}}_s}\{&\boldsymbol{f}_s(k+1, \widehat{\boldsymbol{x}}_d(k+1|k), \widehat{\boldsymbol{x}}_s(k+1|k), \\
&\widehat{\boldsymbol{\theta}}(k+1|k), \boldsymbol{u}(k+1)) = \boldsymbol{0}\}
\end{aligned} \tag{20}$$

$$\widehat{\boldsymbol{\theta}}(k+1|k) = \widehat{\boldsymbol{\theta}}(k|k) \tag{21}$$

$$\boldsymbol{\nu}(k+1) = \boldsymbol{y}(k+1) - \boldsymbol{h}(k+1, \widehat{\boldsymbol{z}}(k+1|k)) \tag{22}$$

$$P(k+1|k) = A_f(k)P(k|k)A_f^T(k) + Q_f(k) \quad (23)$$

$$V(k+1) = H_h(k+1)P(k+1|k)H_h^T(k+1) + R(k+1) \quad (24)$$

$$K(k+1) = P(k+1|k+1)H_h^T(k+1)R^{-1}(k+1) \quad (25)$$

$$\hat{z}(k+1|k+1) = \hat{z}(k+1|k) + K(k+1)\nu(k+1) \quad (26)$$

$$P(k+1|k+1) = P(k+1|k) - P(k+1|k)H_h^T(k+1)V^{-1}(k+1) \times H_h(k+1)P(k+1|k) \quad (27)$$

with initial conditions, $\hat{z}(0|0) = \hat{z}_0$ and $P(0|0) = P_0$. $\mathrm{Sol}_{\hat{x}_s}$ denotes the solution of the static equations for the vector $\hat{x}_s$,

$$H_h(k) = \left.\frac{\partial h(z(k),k)}{\partial z}\right|_{z=\hat{z}(k+1|k)} \quad (28)$$

$P(k+1|k) = E\left\{[z(k+1) - \hat{z}(k+1|k)][z(k+1) - \hat{z}(k+1|k)]^T\right\}$ is the error covariance prior to measurements at time $k+1$,

$P(k+1|k+1) = E\left\{[z(k+1) - \hat{z}(k+1|k+1)][\overline{z}(k+1) - \overline{z}(k+1|k+1)]^T\right\}$ is the error covariance matrix after measurements at time $k+1$,

and $K(k+1)$ denotes the Kalman gain.

One should notice that equations (19)–(27) describing the nonlinear algorithm of Kalman filter are coupled as matrices $A_f(k)$ and $H_h(k)$ are functions of $\hat{z}(k|k)$ and $\hat{z}(k+1|k)$ and should be computed on–line.

The submatrices A_{ij} of the matrix $A_f(k) = \left\{ \vdots A_{ij} \vdots \right\}$ for $i,j = 1,2,3$ are given by

$$A_{11} = \frac{\partial \hat{f}_d}{\partial x_d} \qquad A_{12} = \frac{\partial \hat{f}_d}{\partial x_s} \qquad A_{13} = \frac{\partial \hat{f}_d}{\partial \theta}$$

$$A_{21} = -\left(\frac{\partial \overline{f}_s}{\partial x_s}\right)^{-1} \frac{\partial \overline{f}_s}{\partial x_d}\frac{\partial \hat{f}_d}{\partial x_d} \qquad A_{22} = -\left(\frac{\partial \overline{f}_s}{\partial x_s}\right)^{-1} \frac{\partial \overline{f}_s}{\partial x_d}\frac{\partial \hat{f}_d}{\partial x_s} \quad (29)$$

$$A_{23} = -\left(\frac{\partial \overline{f}_s}{\partial x_s}\right)^{-1} \left(\frac{\partial \overline{f}_s}{\partial x_d}\frac{\partial \hat{f}_d}{\partial \theta} + \frac{\partial \overline{f}_s}{\partial \theta}\right)$$

$$A_{31} = 0 \qquad A_{32} = 0 \qquad A_{33} = I$$

The submatrices Q_{ij} of the matrix $Q_f(k) = \left\{ \vdots Q_{ij} \vdots \right\}$ for $i, j = 1, 2, 3$ are defined by the following expressions

$$Q_{11} = Q_d(k) \qquad Q_{12} = -Q_d(k) \left(\frac{\partial \overline{f}_s}{\partial x_d} \right)^T \left(\frac{\partial \overline{f}_s}{\partial x_s} \right)^{-T} \qquad Q_{13} = 0$$

$$Q_{21} = -\left(\frac{\partial \overline{f}_s}{\partial x_s} \right)^{-1} \frac{\partial \overline{f}_s}{\partial x_d} Q_d(k) \qquad Q_{23} = -\left(\frac{\partial \overline{f}_s}{\partial x_s} \right)^{-1} \frac{\partial \overline{f}_s}{\partial \theta} Q_\theta(k) \tag{30}$$

$$Q_{22} = \left(\frac{\partial \overline{f}_s}{\partial x_s} \right)^{-1} \left[Q_s(k) + \left(\frac{\partial \overline{f}_s}{\partial x_d} \right) Q_d(k) \left(\frac{\partial \overline{f}_s}{\partial x_d} \right)^T + \left(\frac{\partial \overline{f}_s}{\partial \theta} \right) Q_\theta(k) \left(\frac{\partial \overline{f}_s}{\partial \theta} \right)^T \right] \left(\frac{\partial \overline{f}_s}{\partial x_s} \right)^{-T}$$

$$Q_{31} = 0 \qquad Q_{32} = -Q_\theta(k) \left(\frac{\partial \overline{f}_s}{\partial \theta} \right)^T \left(\frac{\partial \overline{f}_s}{\partial x_s} \right)^{-T} \qquad Q_{33} = Q_\theta(k)$$

where

$$\frac{\partial \overline{f}_s}{\partial z} = \left. \frac{\partial f_s}{\partial z} \right|_{z = \widehat{z}(k+1|k)} \qquad \frac{\partial \widehat{f}_d}{\partial z} = \left. \frac{\partial f_d}{\partial z} \right|_{z = \widehat{z}(k|k)}$$

and $(\cdot)^{-T}$ denotes the transposed inverse of $(\cdot)$.

In general, the structure of the modified EKF algorithm (19)–(27) is the same as the one for nonlinear dynamic models (Anderson and More, 1979). However, in details, the main differences are in computing the system matrix, A_f, and the generalized covariance matrix of the system noise, Q_f, according to (29) and (30), respectively. Notice that these matrices should be recalculated at each time step k through the use of the prior estimate $\widehat{z}(k+1|k)$ and the estimate $\widehat{z}(k|k)$.

3. A Statistical Test for Checking the Validity of Model

A variety of statistical tests can be performed on the innovations or residuals to determine the validity of the model used in the filter design (Wilsky *et al.*, 1974; Wilsky, 1976; Chien and Adams, 1976). To test the adequacy of the filter model, the modified Sequential Probability Ratio Test (SPRT) with feedback (Chien and Adams, 1976) has been implemented in our combined analytical model–based and knowledge–based real–time diagnosis system. Below, a brief description of this method will be presented.

3.1. Modified SPRT with Feedback

The SPRT developed by Wald (1947) and then modified by Chien and Adams (1976) is one of the simplest test for the whiteness of the innovation sequences defined as

$$\boldsymbol{\nu}(k+1) = \boldsymbol{y}(k+1) - \boldsymbol{h}(k+1, \hat{\boldsymbol{x}}(k+1|k)) \tag{31}$$

The innovation sequence can be considered as an output for the Kalman filter. If the filter reflects the actual system behavior properly, the innovations sequence is an independent Gaussian random sequence with zero mean and covariance $\boldsymbol{V}(k+1)$ (see equation (24)).

According to the modified SPRT, for each component $\nu_j(k+1), j = 1, 2, ..., M$, of the innovation sequence, the following hypotheses are defined:

H_0: null hypothesis, $\nu_j(k+1)$ is an independent Gaussian random sequence with zero mean and variance $V_{jj}(k+1)$,

H_1: alternative hypothesis, $\nu_j(k+1)$ is an independent random sequence with mean $a_j(k+1)$ and variance $V_{jj}(k+1)$,

where $V_{jj}(k+1)$ denotes the $(j,j)th$ component of the covariance matrix $\boldsymbol{V}(k+1)$ given in (24), and

$$a_j(k+1) = a\sqrt{V_{jj}(k+1)} \tag{32}$$

where a is a positive constant.

The test statistic of Wald's SPRT is defined as the logarithm of the joint likelihood ratio (LLR) function $\lambda_j(k+1)$

$$\lambda_j(k+1) = ln \frac{p(\nu_j(1), \nu_j(2), ..., \nu_j(k+1)|H_1)}{p(\nu_j(1), \nu_j(2), ..., \nu_j(k+1)|H_0)} \tag{33}$$

where $p(\ |\ )$ denotes the conditioned probability. As the innovation sequence $\nu_j(k+1)$, $j = 1, 2, ..., M$ is an independent Gaussian random sequence, the LLR can be evaluated as

$$\lambda_j(k+1) = \sum_{i=1}^{k+1} a_j(i) \left[\nu_j(i) - \frac{1}{2}a_j(i)\right] \Big/ V_{jj}(i) \tag{34}$$

or generated recursively as follows

$$\lambda_j(k+1) = \lambda_j(k) + a\left[\tilde{\nu}_j(k+1) - \frac{1}{2}a\right] \tag{35}$$

with initial condition $\lambda_j(0) = 0$, where $\tilde{\nu}_j(k+1) = \nu_j(k+1)/\sqrt{V_{jj}(k+1)}$ denotes normalized quantity with mean a and variance 1. As the method of Wald's test suffers from an extra time delay in detecting the system degradation, the modified LLR of Chien and Adams (1976) is evaluated as

$$\lambda_j^+(k+1) = \begin{cases} \lambda_j(k+1) & \text{if} \quad \lambda_j(k+1) \geq 0 \\ 0 & \text{if} \quad \lambda_j(k+1) < 0 \end{cases} \tag{36}$$

Then, the decision rule is defined as

$$\begin{array}{lll} \text{if} & \lambda_j^+(k+1) > \lambda_s, & \text{choose } H_1 \\ \text{if} & \lambda_j^+(k+1) < 0, & \text{choose } H_0 \\ \text{if} & 0 \le \lambda_j^+(k) \le \lambda_s, & \text{take another observation} \end{array} \tag{37}$$

where λ_s denotes the upper threshold and can be computed from the following equation

$$T = \frac{2}{a^2}\left(e^{\lambda_s} - \lambda_s - 1\right) \tag{38}$$

for a given mean time between false alarms T. For the same mean time between false alarms, the upper threshold λ_s in the modified SPRT is related to the lower and upper thresholds A and B in Wald's SPRT system by

$$e^{\lambda_s} - \lambda_s - 1 = -\left(B + A\frac{e^B - 1}{1 - e^A}\right) \tag{39}$$

where A and B can be computed from the specified error probabilities for false alarms (α) and missed alarms (β)

$$A = ln\left(\frac{\beta}{1-\alpha}\right), \quad B = ln\left(\frac{1-\beta}{\alpha}\right) \tag{40}$$

The appeal of the application of sequential analysis and information feedback lies in the fact that an on–line recursive technique is more attractive than other approaches.

4. Design of Local Estimators and Application to Fault Detection

In this section, the failure detection of the deaerator control subsystem of a coal–fired power plant is considered based on the analytical redundancy approach. To design local filters, the system shown in Figure 2 is decomposed into: condensate pump, control valve/condensate line, extraction pipe, deaerator, and controller.

The list of faults considered for the deareator control subsystem are

- sensors failures
  - i) deaerator level sensor failure, L
  - ii) condensate flow sensor failure, ω_p
  - iii) deaerator output flow sensor failure, $\omega_{d_{out}}$
- gain faults in the controller
  - i) gain fault of the proportional part, k_p
  - ii) gain fault of the integral part, k_I

- transportation line faults
  - i) valve/condensate line flow conductance, C_{eq}
  - ii) steam flow rate, w_e

To detect the mentioned above faults, the Kalman filter approach will be used. It is resonable to point out that these faults constitute only a portion of the faults considered in our knowledge–based system. The remaining faults are detected using compiled knowledge about the process, and this problem is omitted in this paper. Here we only focus on the detection problems of the above faults.

In many applications of Kalman filter technique for fault detection, the state and/or parameter estimators have been designed for the entire system (Chao and Paolella, 1990). In this work, the system is decomposed into units for which individual filters are formulated. In the following, the design problem of local estimators and their simulation results will be presented. These filter modules which are employed in the knowledge base have been implemented in the software environment of MODEL (Model Software).

4.1. The Condensate Line Failure

A typical fault of the condensate line is caused by the partial pipe plugging which can be detected by the on–line identification of the valve/pipe conductance C_{eq}. To solve this problem, let us assume that the mass flow rate of water leaving pump ω_p and the unknown parameter C_{eq} create the state vector

$$\boldsymbol{z} = [\omega_p \ \ C_{eq}]^T \tag{41}$$

Furthermore, it is assumed that the mass flow rate of water entering valve, ω_p, is the output measurement, with zero mean noise v_ω. Then the process model can be expressed as

$$\omega_p = C_{eq}\left[\overline{\rho}_{pv}(P_p - P_v) + \overline{\rho}_{pv}^2 \Delta H_v/144\right]^{1/2} \tag{42}$$

$$C_{eq}(k+1) = C_{eq}(k) + w_c(k) \tag{43}$$

$$\omega_p = \omega_p + v_\omega \tag{44}$$

where w_c is the parameter model noise, v_w is the measurement noise, and $\overline{\rho}_{pv}$ is assumed to be constant. The process model (42)–(44) is described by both the static equation (42) and the dynamic equation (43).

To design the modified EKF (19)–(27) for the system described by (42)–(44), the static, dynamic, and observation functions take the following form

$$\boldsymbol{f}_d(\cdot) = \boldsymbol{0}, \qquad \boldsymbol{f}_\theta(\cdot) = C_{eq}(k), \qquad \boldsymbol{h}(\cdot) = \omega_p$$

$$\boldsymbol{f}_s(\cdot) = C_{eq}[\overline{\rho}_{pv}(P_p - P_v) + \overline{\rho}_{pv}^2 \Delta H_v/144]^{1/2} - \omega_p \tag{45}$$

The derivates of $\boldsymbol{f}_s(\cdot)$ with respect to ω_p and C_{eq} are given as

$$\frac{\partial \boldsymbol{f}_s}{\partial \omega_p} = -1, \qquad \frac{\partial \boldsymbol{f}_s}{\partial C_{eq}} = [\overline{\rho}_{pv}(P_p - P_v) + \overline{\rho}_{pv}^2 \Delta H_v/144]^{1/2}$$

Thus, the matrix $\boldsymbol{A}_f$ is a (2×2) matrix,

$$\boldsymbol{A}_f = \begin{bmatrix} 0 & a_{12} \\ 0 & 1 \end{bmatrix} \tag{46}$$

where

$$a_{12} = -\left(\frac{\partial \overline{\boldsymbol{f}}_s}{\partial \omega_p}\right)^{-1} \frac{\partial \overline{\boldsymbol{f}}_s}{\partial C_{eq}} = \frac{\partial \overline{\boldsymbol{f}}_s}{\partial C_{eq}}$$

Furthermore, the matrix $\boldsymbol{Q}_f$ is a (2×2) matrix and its elements are

$$q_{11} = \left(\frac{\partial \overline{\boldsymbol{f}}_s}{\partial \omega_p}\right)^{-1} \left[Q_s + \frac{\partial \overline{\boldsymbol{f}}_s}{\partial C_{eq}} Q_\theta \frac{\partial \overline{\boldsymbol{f}}^T}{\partial C_{eq}}\right] \left(\frac{\partial \overline{\boldsymbol{f}}_s}{\partial \omega_p}\right)^{-T} = Q_s + \frac{\partial \overline{\boldsymbol{f}}_s}{\partial C_{eq}} Q_\theta \frac{\partial \overline{\boldsymbol{f}}_s}{\partial C_{eq}}$$

$$q_{12} = -\left(\frac{\partial \overline{\boldsymbol{f}}_s}{\partial \omega_p}\right)^{-1} \frac{\partial \overline{\boldsymbol{f}}_s}{\partial C_{eq}} Q_\theta = \frac{\partial \overline{\boldsymbol{f}}_s}{\partial C_{eq}} Q_\theta \tag{47}$$

$$q_{21} = -Q_\theta \left(\frac{\partial \overline{\boldsymbol{f}}_s}{\partial C_{eq}}\right)^T \left(\frac{\partial \overline{\boldsymbol{f}}_s}{\partial \omega_p}\right)^{-T} = Q_\theta \frac{\partial \overline{\boldsymbol{f}}_s}{\partial C_{eq}} \qquad q_{22} = Q_\theta$$

Note that in this case Q_θ and Q_s are scalars and denote variances of parameter and static model noises, respectively. From the measurement equation (44), we also have that $\boldsymbol{H}_h = [1 \;\; 0]$.

For the valve model (42)–(44), the results are presented in Figures 3–5. The steady state solution for the valve model is $\widetilde{\boldsymbol{z}} = [\widetilde{\omega}_p \;\; \widetilde{C}_{eq}]^T = [3.65 \cdot 10^6 \;\; 2.93 \cdot 10^4]^T$. The measurement noise standard deviation δ_v and the system parameter noise variance δ_s^2 are: $\delta_v = 7.3 \cdot 10^4$, $\delta_s^2 = 10^{-4}$.

Figure 3 represents the behavior of the estimated mass flow rate $\widehat{\omega}_p$ and equivalent conductance $\widehat{C}_{eq}$ when the initial condition for the estimation model ($w_p = 3.65 \cdot 10^6$, $C_{eq} = 2.00 \cdot 10^4$) was considerably different than the "true" steady–state value. The estimates of the flow rate and the conductance approach the true values rather quickly (approximatly after 5–6 sampling times).

In Figures 4 and 5, the deaerator level set point was changed from 120 to 118 *inches*. The system responded to this change by restricting the valve's opening for a period of time. These two cases differ in measurement noise standard deviations ($\delta_v = 7.3 \cdot 10^4$ and $1.46 \cdot 10^4$). The abrupt changes of the conductance occurring at different times are detected well.

4.2. The Condensate Flow Sensor Failure

In general the condensate flow sensor failure can be detected using the mathematical model of the deareator or the condensate line. Taking into account the different complexity of these models, the valve model was chosen. To detect the sensor failure, the valve model (42)–(44) has to be transformed to another form. For this case, the pressure of water leaving pump and entering valve P_p is considered as the new state variable, the mass flow rate ω_p is the unknown parameter, and the pressure P_p is the measured variable. Under these assumptions the "new" valve model can be easily obtained from (42)–(44) in the form of a two–state model $\boldsymbol{z} = [P_p \ \ \omega_p]^T$ as

$$P_p = \frac{\omega_p^2(k)}{C_{eq}^2 \bar{\rho}_{pv}} - \bar{\rho}_{pv} \Delta H_v/144 + P_v \tag{48}$$

$$\omega_p(k+1) = \omega_p(k) + w_\omega \tag{49}$$

with the measurement given by

$$P_p = P_p + v_p \tag{50}$$

where w_ω is the parameter model noise and v_p is the measurement noise.

The structure of the model (48)–(50) is the same as model (42)–(44). In other words, it is given by coupled static and dynamic equations. It is worth to note that the implementation of the modified EKF for the model (48)–(50) gives us the actual behavior of the flow rate $\widehat{\omega}_p(k)$. Thus, upon comparing the output from the filter $\widehat{\omega}_p(k)$ with the output from the actual flow sensor $\omega_p(k)$, we can determine the sensor failure.

To design the modified EKF for the model (48)–(50), we need to write the nonlinear functions describing this process as

$$\boldsymbol{f}_d(\cdot) = 0, \qquad \boldsymbol{f}_\theta(\cdot) = \omega_p(k), \qquad \boldsymbol{h}(\cdot) = P_p$$

$$\boldsymbol{f}_s(\cdot) = \frac{\omega_p^2(k)}{C_{eq}^2 \bar{\rho}_{pv}} - \bar{\rho}_{pv} \Delta H_v/144 + P_v - P_p \tag{51}$$

The derivates of $\boldsymbol{f}_s(\cdot)$ with respect to P_p and ω_p take the form

$$\frac{\partial \boldsymbol{f}_s}{\partial P_p} = -1, \qquad \frac{\partial \boldsymbol{f}_s}{\partial \omega_p} = 2\frac{\omega_p(k)}{C_{eq}^2 \bar{\rho}_{pv}}$$

It is clear that $\boldsymbol{A}_f$ is a (2×2) matrix and has the same structure as (46), with element a_{12} given by

$$a_{12} = -\left(\frac{\partial \bar{\boldsymbol{f}}_s}{\partial P_p}\right)^{-1} \frac{\partial \bar{\boldsymbol{f}}_s}{\partial \omega_p} = \frac{\partial \bar{\boldsymbol{f}}_s}{\partial \omega_p}$$

In turn, the elements of the matrix $\boldsymbol{Q}_f$ are given by

$$q_{11} = Q_s + \frac{\partial \overline{\boldsymbol{f}}_s}{\partial \omega_p} Q_\theta \frac{\partial \overline{\boldsymbol{f}}_s}{\partial \omega_p} \qquad q_{22} = Q_\theta$$

$$q_{12} = \frac{\partial \overline{\boldsymbol{f}}_s}{\partial \omega_p} Q_\theta \qquad q_{21} = Q_\theta \frac{\partial \overline{\boldsymbol{f}}_s}{\partial \omega_p}$$

It is obvious that in this case Q_θ and Q_s are also scalars and the matrix $\boldsymbol{H}_h$ is $\boldsymbol{H}_h = [1 \;\; 0]$.

The effectiveness of the Kalman filter in estimating the pressure P_p and the flow rate ω_p is shown in Figures 6 and 7. Figure 6 shows the estimation results for an initial condition ($P_p = 386.7,\; w_p = 4.3 \cdot 10^6$) that is considerably different than the "true" value. Note that the "true" steady–state solution for the valve model (48)–(50) is $\widetilde{\boldsymbol{z}} = [P_p \;\; \omega_p]^T = [386.7 \quad 3.65 \cdot 10^6]$. In Figure 7, a disturbance was introduced by changing the deaerator level set point from 120 to 118 *inches*. Upon comparing the estimated flow rate with the correct response shown in Figure 4, it is observed that the response of the estimated flow rate is slower than the actual behavior. In both cases, the measurement noise standard deviation δ_v and the system parameter noise variance δ_s^2 are: $\delta_v = 7.72,\; \delta_s^2 = 10^{-4}$.

Finally, one should notice that the condensate flow sensor failure is determined by comparing the filter and sensor outputs.

4.3. The Extraction Pipe Failure

A typical source of fault is low or high steam mass flow rate from the extraction pipe to the deaerator. Thus, information about actual values of the mass flow rate leaving pipe ω_e is important in solving this detection problem. Upon using equation (3) and assuming that the mass flow rate ω_e is the unknown parameter, the desired mathematical model is given by

$$P_e = -\frac{\omega_e^2}{C_f^2 \overline{\rho}_{se}} + \overline{\rho}_{se} \Delta H_{se}/144 + P_s \tag{52}$$

$$\omega_e(k+1) = \omega_e(k) + w_\omega \tag{53}$$

with the measurement equation

$$P_e = P_e + v_p \tag{54}$$

where w_ω is the parameter model noise and v_p is the measurement noise.

It is easily seen that the model (52)–(54) has the same structure as the valve models. Likewise as in subsections 4.1 and 4.2, the modified EKF is used in designing the filter.

From equations (52)–(54), the nonlinear functions are written as

$$f_d(\cdot) = 0 \qquad f_\theta(\cdot) = \omega_e(k) \qquad h(\cdot) = P_e$$

$$f_s(\cdot) = -\frac{\omega_e^2}{C_f^2 \bar{\rho}_{se}} + \bar{\rho}_{se} \Delta H_{se}/144 + P_s - P_e \tag{55}$$

The derivates of $f_s(\cdot)$ with respect to P_e and ω_e take the form

$$\frac{\partial f_s}{\partial P_e} = -1 \qquad \frac{\partial f_s}{\partial \omega_e} = -2\frac{\omega_e}{C_f^2 \bar{\rho}_{se}} \tag{56}$$

In this case, A_f is a (2×2) matrix that has the same structure as (46) with element a_{12} given as

$$a_{12} = \frac{\partial \bar{f}_s}{\partial \omega_e}$$

Furthermore, the elements of Q_f are

$$q_{11} = Q_s + \frac{\partial \bar{f}_s}{\partial \omega_e} Q_\theta \frac{\partial \bar{f}_s^T}{\partial \omega_e} \qquad q_{22} = Q_\theta$$

$$q_{12} = \frac{\partial \bar{f}_s}{\partial \omega_e} Q_\theta \qquad q_{21} = Q_\theta \frac{\partial \bar{f}_s}{\partial \omega_e}$$

The estimation results for this module are shown in Figure 8. In this case, the filter is started from a value ($w_e = 7.5 \cdot 10^5$) that is substantially lower than the actual flow rate ($w_e = 8.5 \cdot 10^5$). As it is seen, the "true" value of the steam mass flow rate is estimated rather quickly and accurately. For this case, the measurement noise standard deviation δ_v and the parameter noise variance δ_s^2 are: $\delta_v = 2.0$, $\delta_s^2 = 10^{-4}$.

4.4. The Gain Faults in the Controller

For the controller, two modules for estimating the proportional gain, k_p, and the integral gain, k_I, are considered using the Kalman filter approach. Note that for models consisting of only dynamic equations, the modified EKF reduces to the nonlinear Kalman filter algorithm.

4.4.1. The Integrator Gain Fault

This problem can be considered as a typical fault diagnosis problem for a system with parametric failure. In this case, the desired state vector is defined as $z = [O_I, k_I]$, where k_I is treated as an unknown parameter to be estimated based on the measured controller output O_T degraded by noise. On using the model equations given in subsection 1.4, the desired discrete–time controller model is described by

$$\begin{aligned} O_I(k+1) &= O_I(k) + \Delta t k_I(k)\{\varepsilon(k) + k_a[\min(O_h - O_T, 0) \\ &\quad + \max(O_l - O_T, 0)]\} \end{aligned} \tag{57}$$

$$k_I(k+1) = k_I(k) + w_k(k) \tag{58}$$

with measurement equation

$$O_T(k) = O_I(k) + k_p\varepsilon(k) + v_o(k) \tag{59}$$

where Δt denotes the sampling time, and

$$\varepsilon(k) = k_1(L_s - L_m(k)) + k_2\omega_{d_{out}}(k) - k_3\omega_c(k) \tag{60}$$

$L_m(k)$, $\omega_{d_{out}}(k)$ and $\omega_c(k)$ are the measured signals. Furthermore, $w_k(k)$ and $v_o(k)$ are noises with known statistics.

To solve the state estimation problem for the controller model (57)–(60), the EKF is used. In accordance with the general description, the elements of the nonlinear function $\boldsymbol{f}_d = [f_1 \quad f_2]^T$ are given by

$$\begin{aligned} f_1(\cdot) &= O_I(k) + \Delta t\ k_I(k)\{\varepsilon(k) + k_a[\min(O_h - O_T, 0) \\ &\quad + \max(O_l - O_T, 0)]\} \end{aligned} \tag{61}$$

$$f_2(\cdot) = k_I(k) \tag{62}$$

and in addition

$$h(\cdot) = O_I(k) + k_p(k)\varepsilon(k) \tag{63}$$

By definition, the matrix $\boldsymbol{A}_f$ has the form

$$\boldsymbol{A}_f = \begin{bmatrix} \dfrac{\partial f_1}{\partial O_I} & \dfrac{\partial f_1}{\partial k_I} \\ 0 & 1 \end{bmatrix} \tag{64}$$

where its elements are

$$\begin{aligned} \frac{\partial f_1}{\partial O_I} &= 1 + \Delta t\ k_I(k)\ k_a \frac{\partial}{\partial O_I}[\min(O_h - O_I - k_p\varepsilon(k), 0) \\ &\quad + \max(O_l - O_I - k_p\varepsilon(k), 0)] \end{aligned}$$

$$\frac{\partial f_1}{\partial k_I} = \Delta t\ \{\varepsilon(k) + k_a\,[\min(O_h - O_T, 0) + \max(O_l - O_T, 0)]\}$$

and the matrix $\boldsymbol{H}_h$ is equal to $\boldsymbol{H}_h = [1 \;\; 0]$.

To test this submodule, a test case was generated. First, it was assumed that a parameter k_I fault occurs at sampling time $k = 34$ by a rise of value from 0.05 to 0.1. Note that it is impossible to estimate the uknown parameter k_I using only the measurement data obtained in the steady–state operation of the system and therefore an additional disturbance should be introduced. In our case, the deaerator level setpoint was changed at $k = 53$ from 120 to 115 *inches*. Figure 9 represents the measured controller output and the estimated values. The measurement noise standard deviation and the system parameter noise variance are $\delta_v = 0.02$, $\delta_s^2 = 10^{-5}$, respectively. The estimation accuracy, or in other words, the detection accuracy of the abrupt change of the integrator gain is quite good.

4.4.2. The Proportional Gain Fault

The proportional gain fault can also be considered as an estimation problem for a dynamic system with an unknown parameter. In this case, the dynamic system defined by equations (10)–(12) can be written in the following discrete form for the unknown proportional gain k_p

$$\begin{aligned} O_I(k+1) &= O_I(k) + \Delta t \; k_I\{\varepsilon(k) + k_a[\min(O_h - O_T, 0) \\ &\quad + \max(O_I - O_T, 0)]\} \end{aligned} \tag{65}$$

$$k_p(k+1) = k_p(k) + w_k(k) \tag{66}$$

with the measured variable

$$O_T(k) = O_I + k_p\varepsilon(k) + v_o(k) \tag{67}$$

To estimate the state vector $\boldsymbol{z} = [O_I, k_p]^T$, we should design a nonlinear filter. The elements of the nonlinear function $\boldsymbol{f}_d = [f_1 \;\; f_2]^T$ are

$$\begin{aligned} f_1(\cdot) &= O_I(k) + \Delta t \; k_I\{\varepsilon(k) + k_a[\min(O_h - k_p(k)\varepsilon(k) - O_I, 0) \\ &\quad + \max(O_l - k_p(k)\varepsilon(k) - O_I, 0)]\} \end{aligned} \tag{68}$$

$$f_2(\cdot) = k_p(k) \tag{69}$$

and the measurement function $h(\cdot)$ is given by (63). Then, the elements of the matrix $\boldsymbol{A}_f$ (equation (64)) are defined by

$$\begin{aligned} \frac{\partial f_1(\cdot)}{\partial O_I} &= 1 + \Delta t \; k_I \; k_a \frac{\partial}{\partial O_I}[\min(O_h - O_I - k_p(k)\varepsilon(k), 0) \\ &\quad + \max(O_l - O_I - k_p(k)\varepsilon(k), 0)] \end{aligned} \tag{70}$$

$$\frac{\partial f_1(\cdot)}{\partial k_p} = \Delta t \; k_I \; k_a \frac{\partial}{\partial k_p} [\min(O_h - O_I - k_p(k)\varepsilon(k), 0) + \max(O_l - O_I - k_p(k)\varepsilon(k), 0)] \tag{71}$$

Furthermore, the matrix $\boldsymbol{H}_h$ is equal to $\boldsymbol{H}_h = [1 \;\; \varepsilon(k)]$.

As in the case of the integrator gain fault detection, a test case was generated. Figure 10 represents the behavior of the estimates and the measured controller output O_T. After the introduction of additional disturbance in the system by the level setpoint change (from 121 to 119 *inches*), the nonlinear filter can detect efficiently the proportional gain fault (a change from 0.1 to 0.05).

4.5. The Level Sensor Failure

The deareator model (6)–(7) is used to solve the level sensor failure in the storage tank. The Kalman filter is designed using the discrete–time deareator model given by

$$h_d(k+1) = h_d(k) + \Delta t h_{d_{cor}}(k) \tag{72}$$

$$P_d(k+1) = P_d(k) - \Delta t \alpha_{hp} h_{d_{cor}}(k) + \Delta t(\omega_{d_{in}} - \omega_{d_{out}})/(V_{tm}\alpha_p) \tag{73}$$

with the measurement equation

$$P_d(k) = P_d(k) + v_p(k) \tag{74}$$

where

$$h_{d_{cor}}(k) = [(-h_d(k) + \gamma\alpha_p^{-1})(\omega_{d_{in}} - \omega_{d_{out}}) + \omega_{d_{in}} h_{d_{in}} - -\omega_{d_{out}} h_{d_{out}}]/[V_{tm}(\rho_d(k) + \gamma\alpha_{hp})]$$

and $v_p(k)$ is the measurement noise with known statistics.

For the dynamic deaerator model (72)–(74), the nonlinear Kalman filter algorithm is applied. The level in the storage tank can then be calculated using the estimates $\widehat{h}_d$ and $\widehat{P}_d$ from the Kalman filter algorithm. Having the state estimates, we can calculate estimates of the bulk density over the entire vessel ρ_d, the density of saturated liquid ρ_f, and the density of saturated vapor ρ_g as follows

$$\widehat{\rho}_d = f_d(\widehat{h}_d, \widehat{P}_d), \qquad \widehat{\rho}_g = f_g(\widehat{P}_d), \qquad \widehat{\rho}_f = f_f(\widehat{P}_d) \tag{75}$$

where $f_d(\cdot)$, $f_g(\cdot)$ and $f_f(\cdot)$ are known steam table functions. Then, the level estimate $\widehat{L}$ can be computed as (see equation (8))

$$\widehat{L}(k) = D\frac{(\widehat{\rho}_d(k) - \widehat{\rho}_g(k))V_t}{(\widehat{\rho}_f(k) - \widehat{\rho}_g(k))V_s} \tag{76}$$

For the deareator model (72)–(74), the elements of the nonlinear function $\boldsymbol{f}_d = [f_1 \;\; f_2]^T$ are

$$f_1(\cdot) \;=\; h_d(k) + \Delta t h_{d_{cor}}(k) \tag{77}$$

$$f_2(\cdot) \;=\; P_d(k) - \Delta t \alpha_{hp} h_{d_{cor}}(k) + \Delta t(\omega_{d_{in}} - \omega_{d_{out}})/(V_{tm}\alpha_p) \tag{78}$$

and the measurement function is $h(\cdot) = P_d(k)$. Now the elements of the matrix $\boldsymbol{A}_f$ are defined as

$$\frac{\partial f_1(\cdot)}{\partial h_d} = 1 + \Delta t \frac{\partial h_{d_{cor}}}{\partial h_d}, \qquad \frac{\partial f_1(\cdot)}{\partial P_d} = \Delta t \frac{\partial h_{d_{cor}}}{\partial P_d}$$

$$\frac{\partial f_2(\cdot)}{\partial h_d} = -\Delta t \frac{\partial}{\partial h_d}(\alpha_{hp} h_{d_{cor}}) \tag{79}$$

$$\frac{\partial f_2(\cdot)}{\partial P_d} = 1 - \Delta t \frac{\partial}{\partial P_d}(\alpha_{hp} h_{d_{cor}}) + \Delta t \left[(\omega_{d_{in}} - \omega_{d_{out}})/V_{tm} \frac{\partial}{\partial P_d} \alpha_p^{-1} \right]$$

and $\boldsymbol{H}_h = [0 \;\; 1]$.

The performance of this filter was found to be poor. A linear time–invariant approximation of the model was used to study the observability properties of the state–space model. The enthalpy was found to have very poor observability behavior. This was revealed through examining both the observability matrix and the observability gramian. The alternative is to use an autoregressive moving average model for the level sensor (Yung and Clarke, 1989).

4.6. The Output Flow Sensor Failure

For the output flow sensor failure, the deareator model (72)–(74) is modified to include the unknown parameter $\omega_{d_{out}}$ as a new state variable. In this case, the deareator model is given by

$$h_d(k+1) \;=\; h_d(k) + \Delta t h_{d_{cor}}(k) \tag{80}$$

$$P_d(k+1) \;=\; P_d(k) - \Delta t \alpha_{hp} h_{d_{cor}}(k) + \Delta t(\omega_{d_{in}} - \omega_{d_{out}})/(V_{tm}\alpha_p) \tag{81}$$

$$\omega_{d_{out}}(k+1) \;=\; \omega_{d_{out}}(k) + w_\omega(k) \tag{82}$$

and the measurement equations are

$$P_d(k) = P_d(k) + v_p(k) \tag{83}$$

$$L(k) = L(k) + v_L(k) \tag{84}$$

The model (80)–(84) is nonlinear and therefore the nonlinear Kalman filter was designed to estimate the enthalpy h_d, the pressure P_d, and the output flow $\omega_{d_{out}}$. The elements of the matrix $\boldsymbol{A}_f$ are

$$A_f = \begin{bmatrix} \frac{\partial f_1(\cdot)}{\partial h_d} & \frac{\partial f_1(\cdot)}{\partial P_d} & \frac{\partial f_1(\cdot)}{\partial \omega_{d_{out}}} \\ \frac{\partial f_2(\cdot)}{\partial h_d} & \frac{\partial f_2(\cdot)}{\partial P_d} & \frac{\partial f_2(\cdot)}{\partial \omega_{d_{out}}} \\ 0 & 0 & 1 \end{bmatrix} \tag{85}$$

The derivatives of f_1 and f_d with respect to h_d and P_d are the same as those given in (79). The remaining elements are

$$\frac{\partial f_1(\cdot)}{\partial \omega_{d_{out}}} = \Delta t \frac{\partial h_{d_{cor}}}{\partial \omega_{d_{out}}}$$

$$\frac{\partial f_2(\cdot)}{\partial \omega_{d_{out}}} = -\Delta t \frac{\partial}{\partial \omega_{d_{out}}} (\alpha_{hp} h_{d_{cor}}) - \Delta t / (V_{tm} \alpha_p) \tag{86}$$

The designed nonlinear Kalman filter for the deareator model (80)–(84) was tested under different initial conditions. Figure 11 shows the estimates of enthalpy, pressure and flow, and the measured pressure when the initial condition of the output flow (i.e., the sensor value; $\omega_{d_{out}} = 2.0 \cdot 10^6$) is lower than the true value ($\omega_{d_{out}} = 4.5 \cdot 10^6$). Figure 12 represents the estimation results when the initial condition of the output flow ($\omega_{d_{out}} = 6.0 \cdot 10^6$) is substantially higher than the true value. The measurement noise standard deviations for the pressure and level and the system parameter noise variance are: $\delta_{v_P} = 0.28$, $\delta_{v_L} = 0.29$, and $\delta_s^2 = 10^{-3}$. In both cases, the accuracy of the estimated flow is good. As stated previously, the sensor failure is detected by comparing the sensor and filter values.

5. Conclusions

We have described an approach of sensor and parameter fault detection for the deareator control subsystem of a power plant. Our main objectives in this paper were to design state estimating filters for sensor and parameter fault detection using the nonlinear Kalman algorithm and the modified EKF. It should be mentioned that the modified Kalman filter for the coupled steady–state and dynamic equations has been proposed by our group (Fathi *et al.*, 1991). In this estimation algorithm, the error covariance matrix prior to current measurements is updated using filtered estimates rather than the predicted quantities. This has an impact on the convergence properties of the algorithm when it is used for parameter estimation. The numerical experiments implemented using the decomposed deaerator control subsystem illustrated the effectiveness of the algorithm for fault detection in power plants. Further research is needed to test the system using real data after the inclusion of low–pressure feedwater heaters between the level controller and the deaerator. Functional redundancy techniques can have major impact on actual power plant operation.

References

Anderson B.D.O. and Moore J.B. (1979): *Optimal Filtering.*– Englewood Cliffs: Prentice Hall.

Bryson J.A.E. and Ho Y.C. (1975): *Applied Optimal Control.*– New York: Hemisphere Publishers.

Chao D. and Paolella P. (1990): *Model–based failure detection and isolation of automotive powertrain systems.*– Proc. Amer. Control Conf., San Diego, v.3, pp.2888–2905.

Chien T.T. and Adams M.B. (1976): *A sequential failure detection technique and its application.*– IEEE Trans. Automat. Control, v.AC–21, pp.750–757.

Davis M.H.A. (1975): *The application of nonlinear filtering to fault detection in linear systems.*– IEEE Trans. Automat. Control, v.AC–20, pp.257–259.

Eckert S., Loparo K. and Roth Z. (1986): *An application of nonlinear filtering to instrument failure detection in a pressurized water reactor.*– Nuclear Technology, v.74, No.2.

Fathi Z., Ramirez W.F. and Aarna O. (1991): *A joint state and parameter estimator for systems with coupled fast and slow dynamic models.*– AIChE Annual Meeting, Los Angeles, Nov.17–22.

Fault Detection, Supervision and Safety for Technical Processes – SAFE-PROCESS'91 (1991): Prep. IFAC/IMACS Symp., Sept. 10–13, Baden–Baden, Germany.

Finch F.E. and Kramer M.A. (1988): *Narrowing diagnostic focus using functional decomposition.*– AIChE Journal, v.34, No.1, pp.25–35.

Frank P.M. (1990): *Fault diagnosis in dynamic systems using analytical and knowledge–based redundancy. A Survey and some new results.*– Automatica, v.26, No.3, pp.459–474.

Gertler J., Costin J., Fang X., Hira R., Kowalczuk Z. and Luo Q. (1991): *Model–based on–board fault detection and diagnosis for automotive engines.*– Prep. IFAC/IMACS Symp. "Fault Detection, Supervision and Safety for Technical Processes" - SAFEPROCESS'91, Baden–Baden, Germany, v.1, pp.241–246.

Gertler J. and Singer D. (1990): *A new structural framework for parity equation–based failure detection and isolation* .– Automatica, v.26, No.2, pp.381–388.

Hengy D. and Frank P.M. (1986): *Component failure detection via nonlinear state observers.*– Proc. IFAC Workshop, "Fault Detection and Safety in Chemical Plants," Kyoto, Japan, pp.153–157.

Isermann R. (1984): *Process fault detection based on modeling and estimation methods. A survey.*– Automatica, v.20, No.4, pp.387–404.

Jazwinski A.H. (1970): *Stochastic Processes and Filtering Theory.*– New York: Academic Press.

Johannsen G. and Alty J.L. (1991): *Knowledge engineering for industrial experts systems.*– Automatica, v.27, No.1, pp.97–114.

Jones H.L. (1973): *Failure Detection in Linear Systems.*– Cambridge: Ph.D. Thesis, MIT, MA.

Kerr T.H. (1977): *False alarm and correct detection probabilities over a time interval for restrieted classes of failure detection algorithm* .– IEEE Trans. Inf. Theory, v.IT–28, No.4, pp.619–631.

Korbicz J. and Zgurovsky M.Z. (1991): *Estimation and Control of Stochastic Distributed Parameter Systems.*– Warsaw: Polish Scientific Publishers.

Korbicz J., Fathi Z. and Ramirez W.F. (1991): *State estimation schemes for fault detection and diagnosis in dynamic systems.* – Appl. Math. & Com. Sci., No.1, v.1, pp.83–106.

Kramer M.A. and Leonard J.A. (1990): *Diagnosis using backpropagation neural networks – Analysis and criticism.*– Computers Chem. Engng., v.14, No.12, pp.1323–1338.

Loparo K.A., Buchner M.R. and Vasudeva K.S. (1991): *Leak detection in an experimental heat exchanger process: A multiple model approach.*– IEEE Trans. Automat. Control, v.36, No.2, pp.167–177.

Loparo K.A., Roth Z.S. and Eckert S.J. (1986): *Nonlinear filtering for systems with random structure.*– IEEE Trans. Automat. Control, v.AC-31, No.1, pp.1064–1067.

Luck R. and Ray A. (1991): *Failure detection and isolation of ultrasonic ranging sensors for robotic applications.*– IEEE Trans. Syst. Man and Cybernetics, v.21, No.1, pp.221–227.

Mehra R.K. and Peschon J. (1971): *An innovations approach to fault detection and diagnosis in dynamical systems.*– Automatica, v.7, pp.637–640.

Miller T., Sutton R.S. and Werbos P.J. (1990): *Neural Networks for Control.*– Cambridge: MIT Press, MA.

Misawa E.A. and Hedrick J.K. (1988): *Nonlinear observers: A state-of-the-art survey.* In *Recent Advances in Control of Nonlinear and Distributed Parameter Systems, Robust Control, and Aerospace Control Applications.*– Benstsman J. and Joshi S.M. (Eds.), New York, pp.59–69.

Model Software. *Solution for Real-Time Simulation and Control.*– 52 Curtis Court, Broomfield, CO 80020.

Naidu S.R., Zafiriou E. and McAvoy T.J. (1990): *Use of neural networks for sensor failure detection in a control system.*– IEEE Control Syst. Mag., v.10, No.3, pp.49–55.

Neumann D. (1990): *A knowledge based fault diagnosis system for the supervision of periodically and intermittent working machine tools.*– Proc. 11th IFAC Congress, Tallinn, USSR, pp.135–140.

Patton R. and Chen J. (1991): *A review of parity space approaches to fault diagnosis.*– Prep. IFAC/IMACS Symp. "Fault Detection, Supervision and Safety for Technical Processes" – SAFEPROCESS'91, Baden- -Baden, Germany, v.1, pp.239–255.

Patton R., Frank P. and Clark R. (1989): *Fault Diagnosis in Dynamic Systems. Theory and Applications.*– New York: Prentice Hall.

Prock J. (1991): *A new technique for fault detection using Petri nets.*– Automatica, v.27, No.2, pp.239–245.

Sorenson H.W. (Ed.) (1985): *Kalman Filtering: Theory and Application.*– New York: IEEE Press.

Sorsa T. and Koivo H.N. (1991): *Application of artificial neural networks in process fault diagnosis.*– Prep. IFAC/IMACS Symp. "Fault Detection, Supervision and Safety for Technical Processes" – SAFEPROCESS'91, Baden–Baden, Germany, v.2, pp.133–142.

Tsuge Y., Ikeda K., Shibata and Matsuyama H. (1991): *Hierarchical fault diagnosis system utilizing the signed directed graph and the extended Kalman filter.*– Prep. IFAC/IMACS Symp. "Fault Detection, Supervision and Safety for Technical Processes" – SAFEPROCESS'91, Baden–Baden, Germany, v.1, pp.153–158.

Tylee J.L. (1982): *A generalized likelihood ratio approach to detecting and identifying failures in pressurizer instrumentation.*– Nuclear Technology, v.56, pp.484–493.

Tzafestas S.G. (Ed.) (1989): *Knowledge-Based System Diagnosis, Supervision, and Control.*– New York, London: Plenum.

Wald A. (1947): *Sequential Analysis.*– New York: John Wiley.

Watanabe K. and Himmelblau D.M. (1982): *Instrument fault detection in systems with uncertainties.*– Int. J. Syst. Sci., v.13, No.2, pp.137–158.

Watanabe K. and Himmelblau D.M. (1983): *Fault diagnosis in nonlinear chemical processes.*– Part I. *Theory.*– AIChE Journal, v.29, No.2, pp.243–249. Part II. *Application to a chemical reactor.*– AIChE Journal, v.29, No.2, pp.250–260.

Willsky A.S. (1976): *A survey of design methods for failure detection in dynamic systems.*– Automatica, v.12, pp.601–611.

Willsky A.S., Deyst J.J. and Crawford B.S. (1974): *Adaptive filtering and self-test methods for failure detection and compensation.*– Proc. of the 19th JACC, Austin, Texas, USA, Une 19–21, pp.637–649.

Willsky A.S. and Jones H.L. (1976): *A generalized likelihood ratio approach to the detection and estimation of jumps in linear systems.*– IEEE Trans. Automat. Control, v.AC–21, pp.108–113.

Wunnenberg J. and Frank P.M. (1990): *Dynamic model–based incipient fault detection concept for robot.*– Proc. 11th IFAC World Congress, Tallinn, Estonia, USSR, pp.1420–1426.

Yao S.Ch. and Zafiriou E. (1990): *Control system sensor failure detction via networks of localized receptive fields.*– Proc. Amer. Control Conf., San Diego, USA, May 23–25, v.3, pp.2472– 2477.

Yoshimura T., Watanabe K., Konish K. and Soeda T. (1979): *A sequential failure detection approach and the identification of failure detection approach and the identification of failure parameters.*–Int. J. Syst. Sci., v.10, No.7, pp.827–836.

Yung S.K. and Clark D.W. (1989): *Local sensor validation.*– Measurement and Control, v.22, pp.132–141.

* This paper partly was prepared during Korbicz's stay at the Department of Chemical Engineering of the University of Colorado at Boulder, U.S.A., sponsored by the IREX.
** This work partly was supported by the State Committee for Scientific Research under grant No.7–1086 91 01.

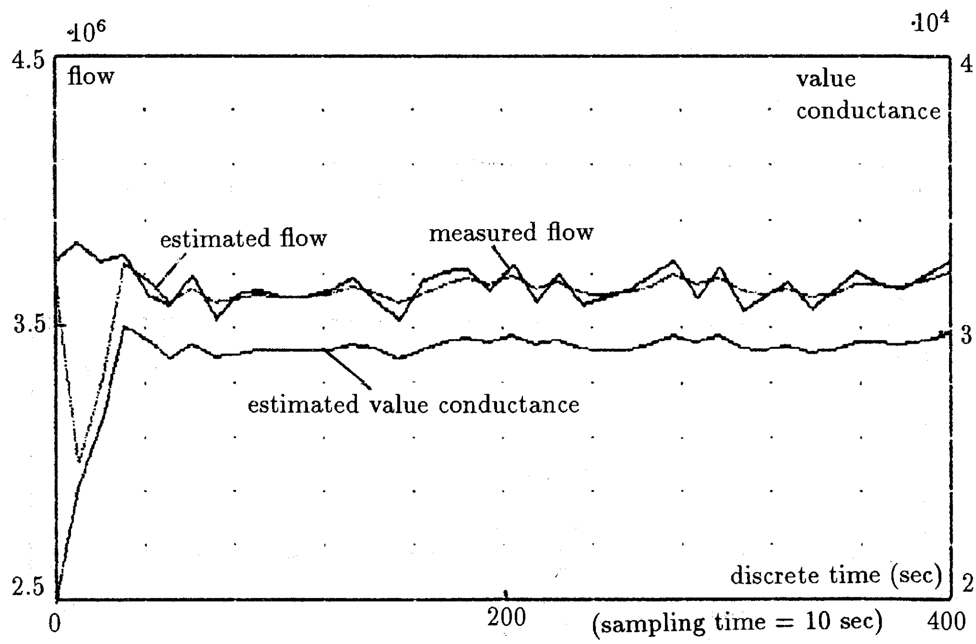

Fig. 3.

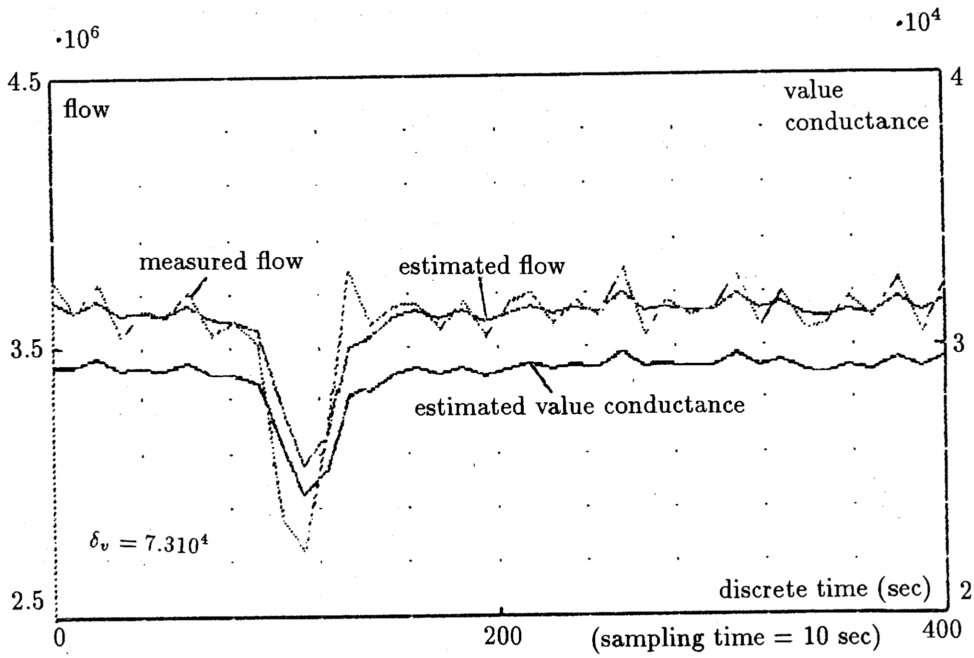

·10^6
·10^4
4.5
4
flow
value
conductance
measured flow
estimated flow
3.5
3
estimated value conductance
$\delta_v = 7.310^4$
2.5
discrete time (sec)
2
0
200
(sampling time = 10 sec)
400

Fig. 4.

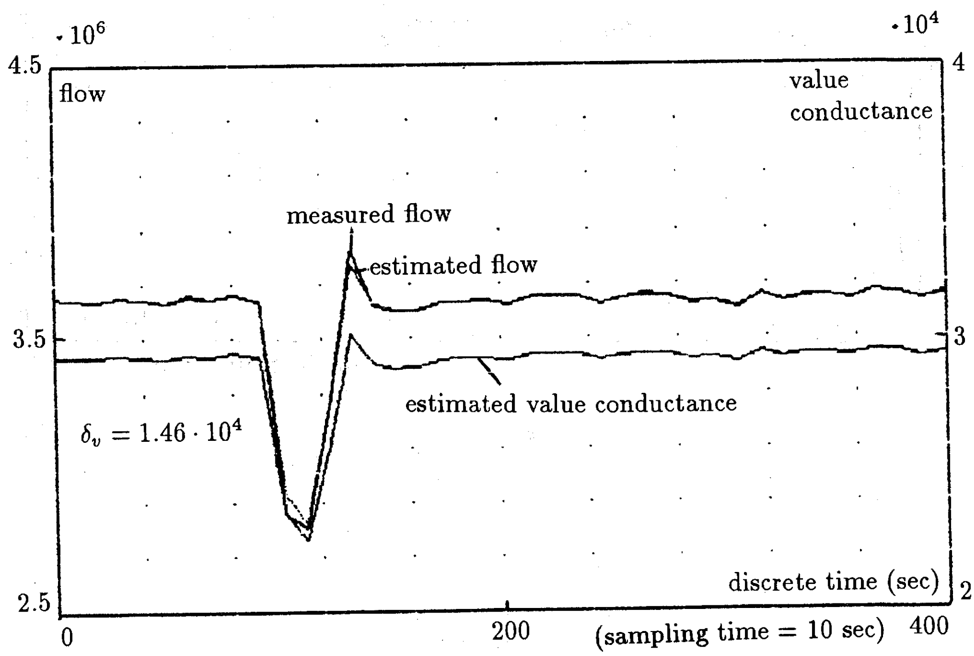

· 10^6
·10^4
4.5
4
flow
value
conductance
measured flow
estimated flow
3.5
3
estimated value conductance
$\delta_v = 1.46 \cdot 10^4$
2.5
discrete time (sec)
2
0
200
(sampling time = 10 sec)
400

Fig. 5.

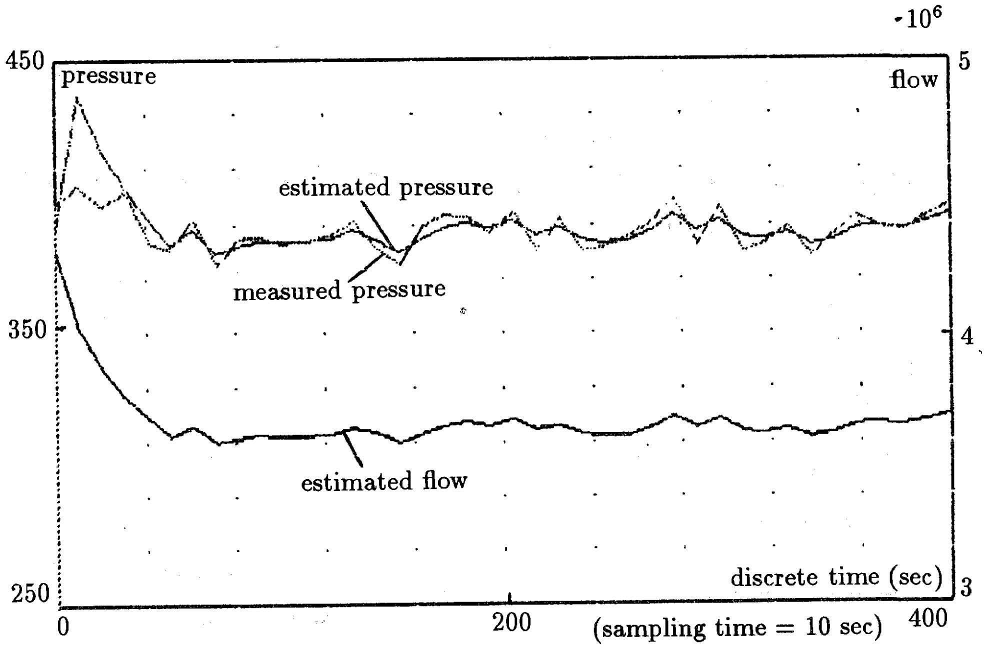

·10^6
450
350
250
5
4
3
pressure
flow
estimated pressure
measured pressure
estimated flow
discrete time (sec)
0
200
400
(sampling time = 10 sec)

Fig. 6.

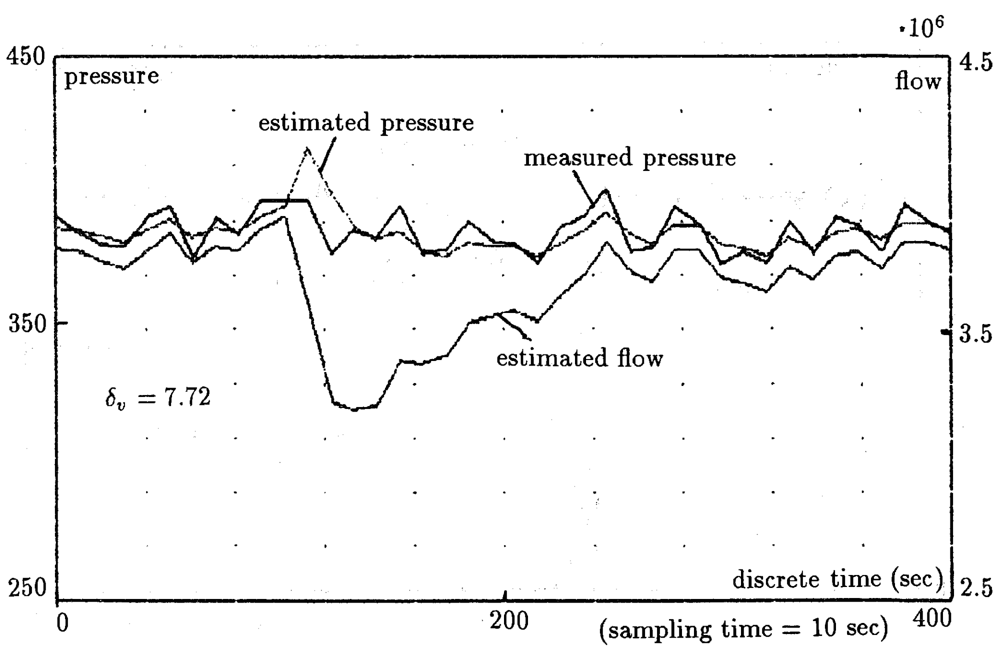

·10^6
450
350
250
4.5
3.5
2.5
pressure
flow
estimated pressure
measured pressure
estimated flow
$\delta_v = 7.72$
discrete time (sec)
0
200
400
(sampling time = 10 sec)

Fig. 7.

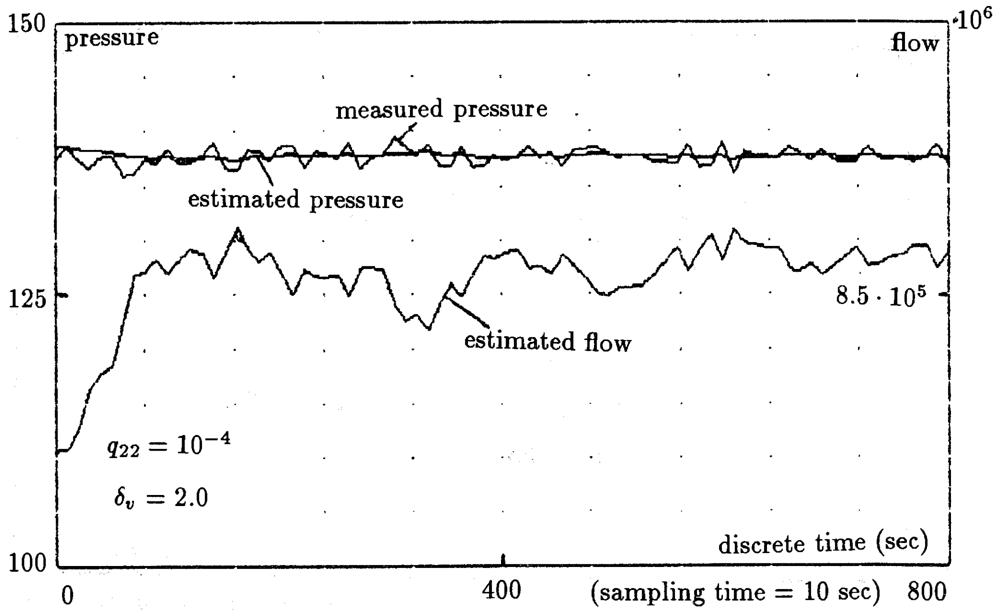
150
125
100
·10^6
pressure
flow
measured pressure
estimated pressure
estimated flow
8.5 · 10^5
$q_{22} = 10^{-4}$
$\delta_v = 2.0$
discrete time (sec)
0
400
(sampling time = 10 sec)
800

Fig. 8.

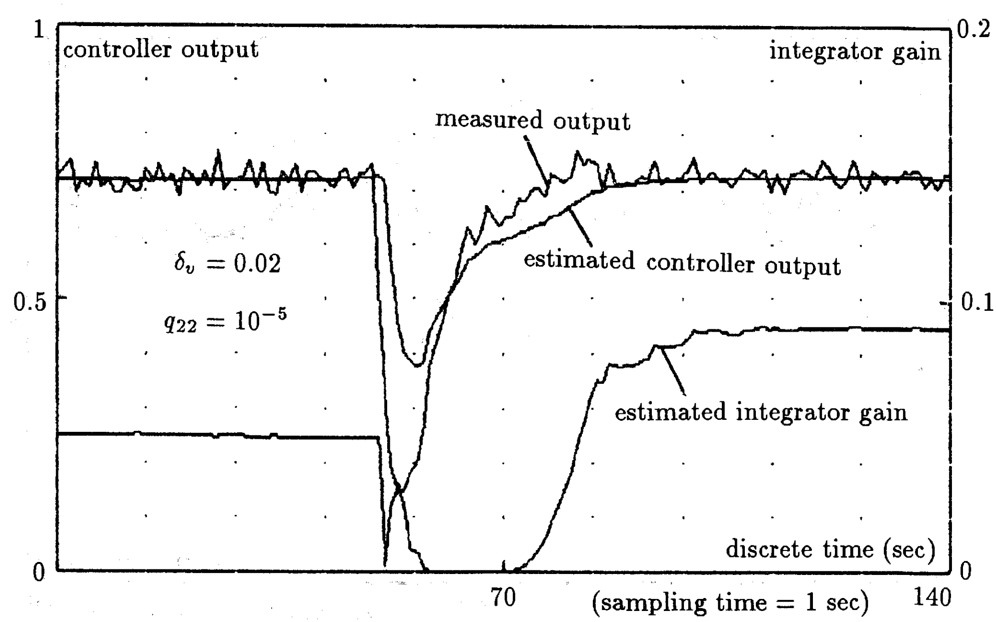
1
0.5
0
0.2
0.1
0
controller output
integrator gain
measured output
estimated controller output
estimated integrator gain
$\delta_v = 0.02$
$q_{22} = 10^{-5}$
discrete time (sec)
70
(sampling time = 1 sec)
140

Fig. 9.

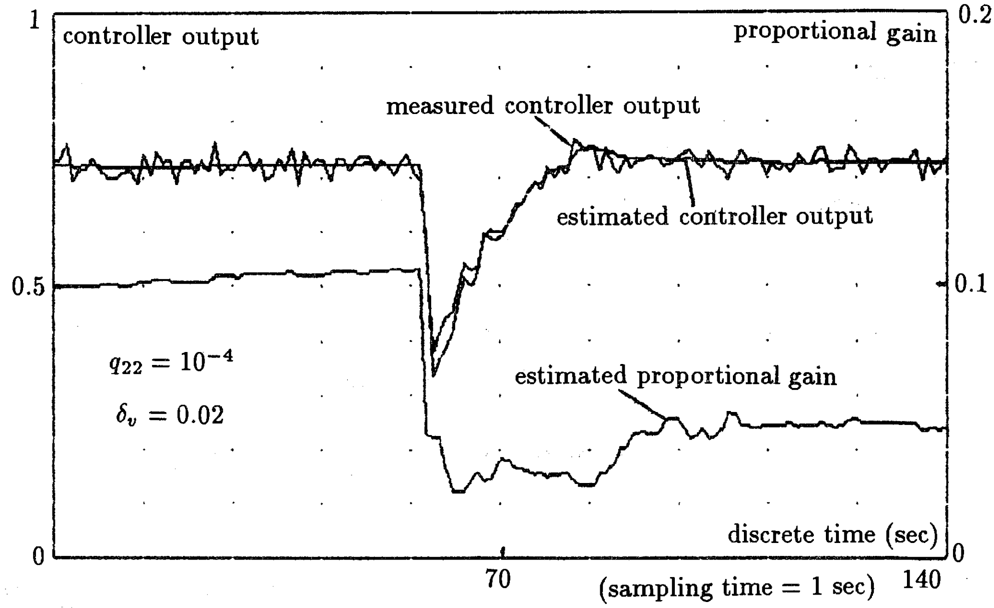

1
0.5
0
0.2
0.1
0
controller output
proportional gain
measured controller output
estimated controller output
$q_{22} = 10^{-4}$
$\delta_v = 0.02$
estimated proportional gain
discrete time (sec)
70
140
(sampling time = 1 sec)

Fig. 10.

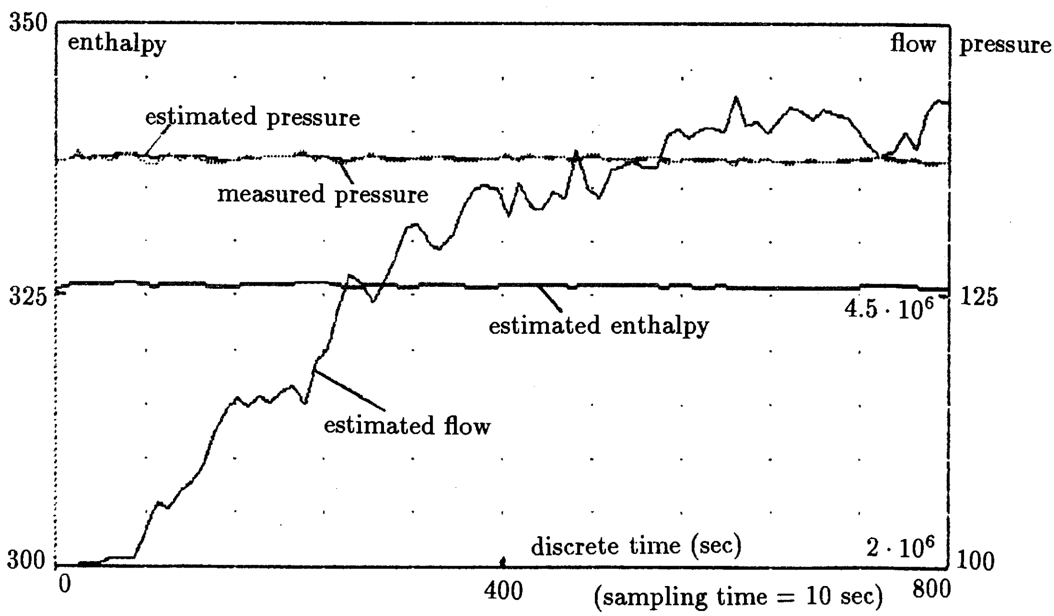

350
325
300
enthalpy
flow
pressure
estimated pressure
measured pressure
estimated enthalpy
$4.5 \cdot 10^6$
125
estimated flow
discrete time (sec)
$2 \cdot 10^6$
100
0
400
800
(sampling time = 10 sec)

Fig. 11.

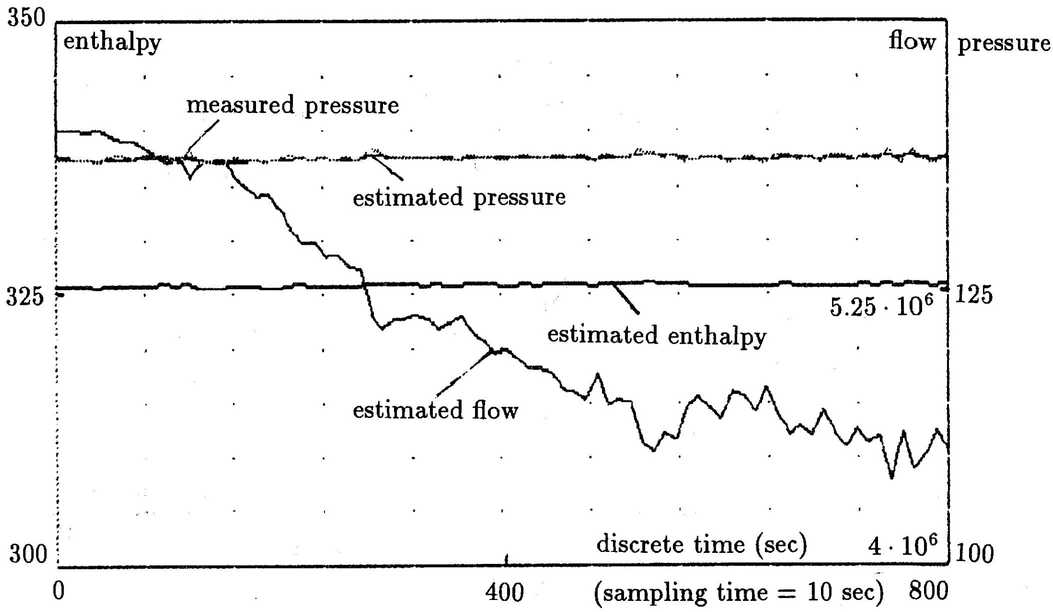
350
enthalpy
flow
pressure
measured pressure
estimated pressure
325
125
$5.25 \cdot 10^6$
estimated enthalpy
estimated flow
300
discrete time (sec)
$4 \cdot 10^6$
100
0
400
(sampling time = 10 sec)
800

Fig. 12.